Stanford Exploration Project, Report 113, July 8, 2003, pages 139–145

Operator aliasing in wavefield continuation migration

Brad Artman, Jeff Shragge, and Biondo Biondi[1]

ABSTRACT

With the widespread adoption of wavefield continuation methods for prestack migration, the concept of operator aliasing warrants revisiting. While zero-offset migration is unaffected, prestack migrations reintroduce the issue of operator aliasing. Some situations where this problem arises include subsampling the shot-axes to save shot-profile migration costs and limited cross-line shot locations due to acquisition strategies. These problems are overcome in this treatment with the use of an appropriate source function or band-limiting the energy contributing to the image. We detail a synthetic experiment that shows the ramifications of subsampling the shot axis and the efficacy of addressing the problems introduced with our two approaches. Further, we explain how these methods can be tailored in some situations to include useful energy residing outside of the Nyquist limits.

INTRODUCTION

Imaging the subsurface by migration of seismic data may give rise to aliasing problems that can generate artifacts in the final image. In Kirchhoff migration, effective solutions to the problem of operator aliasing have been developed and widely implemented by practitioners (Silva, 1992; Lumley et al., 1994; Sun and Bernitsas, 1999). However, wavefield continuation migration is often considered unaffected by operator aliasing, which is only true for zero-offset applications. Accordingly, with the increasing use of prestack wave-equation migrations, it is important to understand the ramifications of data-space sampling choices on the potential aliasing of the image-space.

Aliasing can arise in wave-equation migration during the application of the imaging condition even when propagating wavefields are alias free. Imaging condition aliasing, as discussed by Zhang et al. (2003), occurs when the image space is inappropriately discretized. We address an aliasing problem that arises when, during the application of the imaging condition, wavenumbers improperly map into the image-space due to sampling changes of the data axes. This situation is analogous to the operator aliasing problem in Kirchhoff migration (Biondi, 2001).

We identify two methods of removing aliased energy from the image-space. We derive the criteria for determining the appropriate Nyquist boundaries for the image due to subsampling a

[1]**email:** brad@sep.stanford.edu, jeff@sep.stanford.edu, biondo@sep.stanford.edu

data axis. To illustrate these ideas we present a simple case where aliased energy is introduced into the image due to subsampling the shot axis, and show the efficacy of our methods in removing these artifacts. Two important applications are readily identified: 1) calculating the dip information sacrificed when migrating a decimated data set to save computational costs; and 2) optimizing acquisition direction over complex targets in marine towed array surveys.

METHODOLOGY

To demonstrate how operator aliasing arises, it is informative to study an example where improper sampling generates artifacts in the image. When analyzing this problem, it is common to superpose the shot-receiver ,sr, and location-offset, xh, axes. The definition of the transformation between the coordinate pairs dictates how the movement of energy in one frame is related to changes in the other. Even though there is only rotation between the two coordinate systems, the act of overlaying them on the same Cartesian grid inappropriately applies a stretch of $\sqrt{2}$ and gives rise to confusion especially when trying to interpret the Fourier duals of these dimensions. Therefore, these axis are treated separately in this analysis.

Figure 1 explains how we will visualize distributions of energy in the image-space. By transforming the surface location and CIG-offset axes, (x,h), to the Fourier domain variables, (k_x,k_h), we can view the spatial energy components of the image at a reflector depth. The shaded box in the center of each diagram represents the energy delimited by the Nyquist wavenumbers. The thick line at $k_x = 0$ is the 2-D Fourier transform in the (x,h)-coordinate system of the image at the depth of a flat reflector. Outside of the shaded region the periodicity of Fourier spectrum, due to discrete sampling, is depicted by two of an infinite number of possible Nyquist replicas (dashed lines). Note that the juxtaposition of all of the replications gives rise to the lines of continuous horizontal energy (dot-dash lines).

In panels a and b, which are the data-space and image-space coordinate representations of energy spectra, sampling requirements are honored and no aliasing occurs. The first set of horizontal energy replications will be the first aliased energy to enter the shaded region if an axis is compressed by decimating the data. In our experiments, we have focused on subsampling the shot-axis as indicated by the filled arrows pointing toward the origin. Panels c and d depict the effects of subsampling the shot axis by a factor of two. The replicated energy bands are compressed toward the origin by a factor of two relative to the overlying panels. The energy in the right and left columns moves to the same wavenumber values on their respective axes, despite the rotation of the Nyquist boundaries. Although aliased energy has now moved below Nyquist on the (k_s,k_r)-plane, the replicated $k_x = 0$ energy is now coincident with the Nyquist boundaries on the (k_x,k_h)-plane. However, in the presence of dipping energy ($k_x \neq 0$) aliasing will arise with this degree of subsampling.

We consider two approaches to control the aliasing problems associated with the acquisition and subsampling situations mentioned above. First, wavenumbers from the source and receiver wavefields are band-limited to prevent the entry of aliased duplications into the imaging condition. This does not require eliminating these components from the propagating wavefields, as we can save appropriate portions of the wavefields in disposable buffers for imaging.

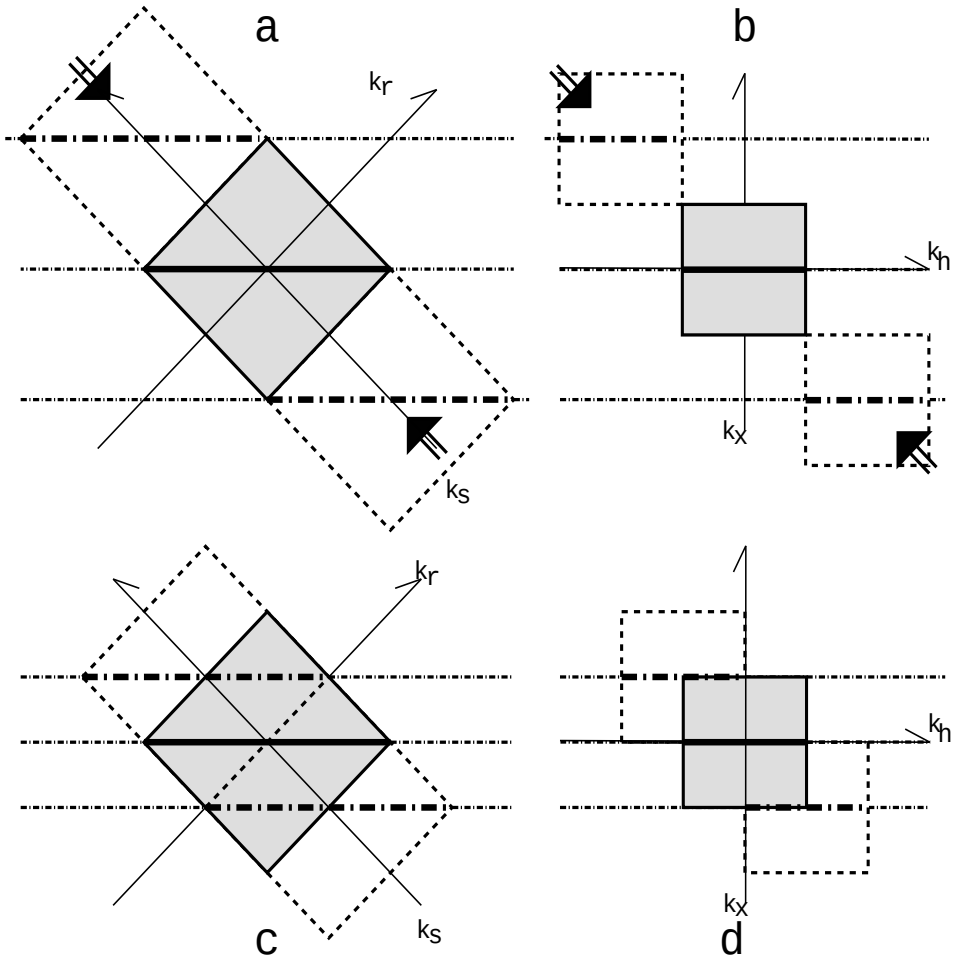

Figure 1: Cartoon illustrating a sample energy distribution in the image-space and the hypothetical position of Fourier domain replications (dotted lines) outside of Nyquist boundaries (shaded region). Dot-dashed lines represent replicated energy from the $k_x = 0$ band of energy corresponding to a single flat reflector at this image depth. Panels (a) and (c) depict the energy components of the data-space. Panels (b) and (d) depict the energy components of the image-space. The bottom row shows the result of a compression along the k_s-axis (indicated by the filled arrows) as a result of migrating every other available shot-location. brad1-scheme [NR]

Second, a band-limited source function is propagated for the duration of each shot-gather migration which effectively zeros energy in the aliased band during imaging. This method manufactures a source function with a wavenumber spectrum limited to the cutoff frequencies imposed by the resampled data axis. There is no additional computational overhead when anti-aliasing with a thick source function, though anti-aliasing by restricting the wavenumbers requires two additional Fourier transforms.

The analytical band-limit is required to appropriately delimit non-aliased wavenumbers for either method. After compression of either data axis, the stretch factor to show the movement of wavenumbers in the (k_x, k_h)-plane is,

$$\text{BandLimit}(k_x) = \frac{max(\Delta r, \Delta s)}{max(a\Delta r, b\Delta s)} min(Ny_r, Ny_s) \tag{1}$$

where $(\Delta r, \Delta s)$ are the original receiver and source increments, (a,b) are the down-sampling ratios from the original to the new receiver and source grids, and (Ny_r, Ny_s) are the original Nyquist limits of the data-space. The *max* functions in the expression are required because the maximum grid-spacing along either shot or receiver axis alone dictates the aliasing criteria for the k_x-axis.

The band-limit value calculated with equation (1) is the criteria for eliminating all energy external to the new rigorously defined Nyquist limit. However, if the dipping energy in the data is limited to less than Nyquist, the maximum dip, $|p|_{max}$, may be used to relax the band-limiting criteria resulting in the definition:

$$\text{BandLimit}(k_x, |p|_{max}) = \frac{Ny_x - |p|_{max}/2}{max(a\Delta r, b\Delta s)}. \tag{2}$$

Note that if the energy distribution is asymmetric (i.e. $p_{min} \neq -p_{max}$), two one-sided limits can be implemented. In the case of only zero dip, the band-limit wavenumber restriction is twice the rigorous definition from equation (1).

EXPERIMENT

A synthetic data set was generated to test these methods of preventing aliasing. Shot-gathers were modeled over a $2000m/s$ earth model with one flat reflector at $1000m$. Nominal shot, Δs, and receiver, Δr, spacing is $10m$. Dominant frequency of the wavelet is $30Hz$. These experiments were performed using a shot-profile algorithm. However, these analyses and conclusions are valid for both shot-geophone and shot-profile migrations due to their mathematical equivalence (Biondi, 2003),(Shan and Zhang, 2003).

The introduction of aliasing artifacts is seen by comparing the panels in Figure 2 constructed at the depth of the reflector. Panels share the characteristics of Figure 1d, though a frequency axis is now introduced by postponing the summation of frequencies normally required by wave-equation migration imaging conditions. Migrating shot-profiles at every receiver location (left panel) shows marked difference to the wavenumber components that make

up the image produced by migrating shots at every tenth shot (center panel). As the $k_x = 0$ energy moves into the image from the replicated Fourier spectra, bands of aliased energy appear at multiples of $10m^{-1}$ on the k_x axis . Both images were constructed with standard shot-profile migration using a single trace source function.

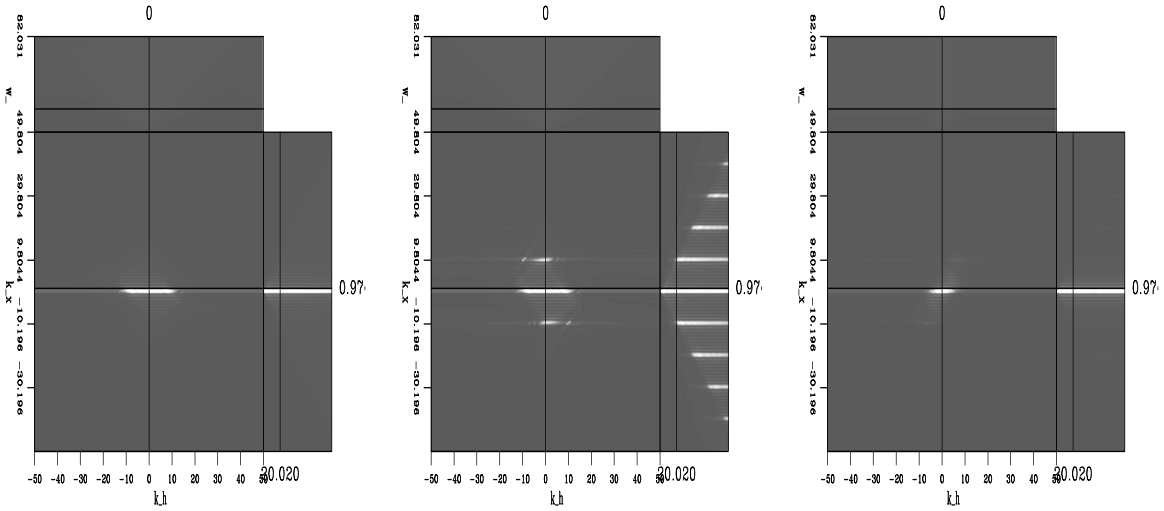

Figure 2: Panels show image wavenumbers from migrations of different selections of available shots from the data set. Left panel was created by migrating all available shots, while the center and right panels include only every tenth shot. Note the replication of the flat reflector at $k_x = 2iNy/10$ in the center panel. The right panel is the result of restricting the migrated energy with a fat source function. Notice that the length of the reflector energy along the $k_x = 0$ axis has been limited from $10m^{-1}$ to $5m^{-1}$ indicating an imposed restriction on the number of offsets contributing to the image at any given dip. Selective energy imaging yields an identical result to the fat wavelet result. brad1-allv10vfat10 [CR]

The right panel, also produced using every tenth shot, illustrates the effectiveness of our methods in eliminating the aliased energy introduced by subsampling the shot axis. The image does not suffer from aliased energy due to the use of a spatially band-limited (fat) source function. It also shows a diminished k_h bandwidth as a result of removing the aliased energy.

Selective energy imaging, our second proposed method, uses band-limited versions of the source and receiver wavefields in the imaging condition. The resultant image is identical to the right panel and is accordingly not shown.

CONCLUSIONS

We conclude that operator aliasing artifacts are indeed introduced during prestack wavefield continuation migration when s- or r-axes are allowed to deviate from a regular grid. This problem is thus manifest both when we choose to subsample the number of shots available from the data or design a survey without shots at every receiver location (or in reciprocal cases

like OBC surveys). We have shown two methods for eliminating aliased contributions to the image.

We feel that it is more appropriate to use selective energy imaging conditions rather than a fat source function. In practice, lateral velocity variation will cause energy constituents in the fk-plane to move around. To allow for any beneficence from this movement, it would be unwise to propagate a band-limited source function, or worse, to eliminate energy from the source and receiver wavefields during propagation steps. Therefore we recommend migrating individual shots on the fine grid, and accounting for image aliasing in the imaging step rather than propagating data decimated to match the grid of the subsampled shot axis (or vice-versa).

With some knowledge of the dip content of the data it is possible to extend the boundaries of anti-aliasing limit criteria. Using both positive and negative one-sided band-limits can allow for the inclusion of appropriate energy into the image that resides outside of the rigorously defined Nyquist boundaries. Therefore, when challenged with imaging important steeply dipping targets, decisions concerning acquisition design or the level of decimation along different directions for migration can be made with a better understanding of the consequences to the final product.

REFERENCES

Biondi, B., 2001, Kirchhoff imaging beyond aliasing: Geophysics, **66**, no. 2, 654–666.

Biondi, B., 2003, Equivalence of source-receiver migration and shot-profile migration: Geophysics, accepted for publication.

Lumley, D. E., Claerbout, J. F., and Bevc, D., 1994, Anti-aliased Kirchhoff 3-D migration: SEP–**80**, 447–490.

Shan, G., and Zhang, G., 2003, Equivalence between shot-profile and source-receiver migration: SEP–**113**, 121–126.

Silva, R., 1992, Antialiasing and the application of weighting factors in Kirchhoff migration: 62nd Ann. Internat. Mtg, Soc. Expl. Geophys., Expanded Abstracts, 995–998.

Sun, J., and Bernitsas, N., 1999, Antialiasing operator dip in 3D prestack Kirchhoff time migration - an exact solution: 61st Mtg., Eur. Assn. Geosci. Eng., Expanded Abstracts, Session:1052.

Zhang, Y., Sun, J., and Gray, S., 2003, Aliasing in wavefield extrapolation prestack migration: Geophysics, **68**, no. 2, 629.